CHAPTER 1 Introduction

Bandpass filters are important components in wireless communication systems, used for filtering the signals that are not wanted and providing transmission at the desired frequency. Due to their wildly application in the wireless communication systems, the filters with small size, low cost and high performance are seriously attractive. The fact that communication systems go smaller and lighter is another motivation of the filter design. If the bandpass filter can be integrated with active components by inserting all external filter components into the transceiver chip, the cost of the system will be greatly reduced.

In this thesis a bandpass filter based on the structure which using short–ended coupled line with lumped capacitors is introduced. The compacted size and the surrounding ground structure enable it can be inserted into the transceiver systems. In addition, the high quality factor (Q) and the relatively stable center frequency are other advantages. The filter can be fabricated using the standard CMOS process.

1.1 An introduction to the filters at present

To meet the demand of some certain applications, the size reduction of filter is of primary importance. Smaller filters are desirable, even though reducing the size of a filter generally leads to reducing

performance. Many efforts have been done on reducing the size of the conventional filters. So far, numerous new filter configurations become possible. For instance, the miniature dual-mode resonator filters [1]-[3] can reduce the filter by half. Slow-wave resonator filter [4], [5] is another effective approach in reducing the size of the bandpass filter by making use of the slow-wave effect in periodic structures. Combline filters using low temperature co-fired ceramic (LTCC) or ceramic materials with the multi-layer technology can be an effective size reduction method [6], [7]. But conventionally the electrical length has been recommended by 45 degree. There are many other size reduction methods such as the hairpin resonator filters [8] and the step impedance filters (SIR) [9]-[11]. All these methods mentioned above can achieve relatively compact bandpass filter size. But still take up a large circuit space. It is inconvenient for the system integration.

Recently, CMOS bandpass filters for a single RF transceiver chip have been driven by reducing the cost and decreasing the RF system design time. A CMOS-based integrated filter using lumped inductors was fabricated [12]. However, the filter design is not convenient and has limitations since the lumped inductor has a complex equivalent circuit and low self-resonance frequency. Active bandpass filter can be an effective approach on size reduction. Great efforts have been done in the area of on-chip active bandpass filter. However, their uptake for commercial RF front end designs is limited owing to the poor performances resulting from the low quality factor of monolithic spiral inductors. These inductors suffer inherently from a variety of energy dissipation mechanisms. The Ohmic loss is unavoidable as the primary inductor current flows through

the thin metals of the spiral. Displacement current losses within the dielectric between the inductor and the underlying semiconductor substrate, and eddy current losses within the silicon (Si) substrate [13], [14]. Many approaches have been proposed to solve or alleviate these lossy inductor issues. Such as use patterned ground shields with polysilicon [15] and multi-metal spiral inductors [16], [17]. However, the realization of high quality factors (>10) still remains a challenge using the standard CMOS process. A series of active filters could be used to compensate for the inductor losses, but this approach suffers with other problems such as limited dynamic range, narrow bandwidth, high intermodulation distortion, high noise figure and poor in-band flatness. It has been reported that the system performance using the silicon-on-isolator (SOI) process (where inductors with quality factors Q > 20 are attainable) was comparable to that of a conventional low noise amplifier with an off-chip bandpass filter [18]. However, it is not usual for a single chip transceiver to include an integrated bandpass filter. In spite of its small silicon area and good insertion loss of the active filters, the active circuit has a drawback inherent that it has nonlinear and poor noise characteristics and consumes the DC power. Until recently, there have been limited publications regarding low GHz band, CMOS passive filters.

In this thesis, a novel bandpass filter was designed using the diagonally short-ended coupled line with loaded lumped capacitor for size reduction. The structure is simple and it is convent to integrate with active components. In order to enhance the quality factor, multilayer conductors were used to the coupled line. And the measured result confirmed that the quality factor of the multilayer circuit was much better than the one layer

circuit's. The extraction procedure of Q factors from measurements of miniaturized coupled-line BPFs will be described based on theoretical circuit analysis. The Q factors of the equivalent distributed inductors implemented using the standard CMOS process will be compared with other types of filters. As another advantage of the bandpass filter, it is proved has relatively stable center frequency when the substrate permittivity changes. It means the out circumstances, such as the package, hardly have an impact on it. The mathematical proving and the simulation results were provided to support the fact.

1.2 Organization of the thesis

The contents of the thesis are as follows:

Chapter 1 depicts the background and purpose of this work and give a briefly introduces to the outline of the thesis.

Chapter 2 introduces the design theory of the bandpass filters.

Chapter 3 the simulation and the measurement results are plotted, including simulation in HFSS and measurements. Analyses of the results are showed here.

Chapter 4 draws the conclusion of this work.

CHAPTER 2 The Bandpass Filter Design Theory

There are many traditional bandpass filter structures, such as the end-coupled microstrip bandpass filter, interdigital bandpass filter. Since the parallel coupled-line microstrip filter was proposed by Cohn in 1958 [19], it has been widely used in microwave applications. Due to its strong advantages such as planar structure, simple synthesis procedures and fabrication facility, it becomes an important component in bandpass filter design. However, as the development of the mobile communication, these conventional parallel coupled-line filters are too large to insert into the mobile systems. Many approaches had been developed for miniaturizing the coupled line. In this chapter, the basic theory of this thesis that based on capacitive loading of diagonally short-ended coupled-line for miniaturizing will be introduced.

2.1 Size reduction method

As is well known, a quarter-wave transmission line can be miniaturized to a short line with electrical length of θ, using combinations of shortened transmission line and shunt lumped capacitors proposed by Hirota [20] as shown in Fig. 2.1. The related equations are as follows,

$$Z = Z_0 / \sin\theta \tag{2.1}$$

$$\omega C_1 = (1/Z_0)\cos\theta \tag{2.2}$$

where Z , Z_0 , θ and ω are the characteristic impedance of the shortened transmission line, the characteristic impedance of the quarter-wavelength line, the electrical length of the shortened line.

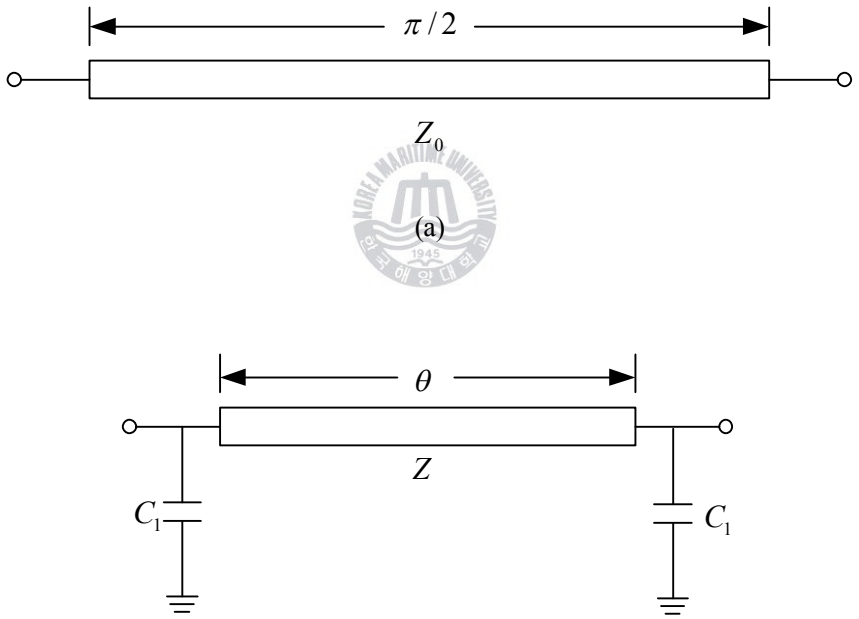

Fig. 2.1 Quarter-wave transmission line (a) and the shortened transmission line with lump capacitors (b).

From (2.1), it is clear that the characteristic impedance of the

shortened transmission line Z goes higher as the electrical length θ goes smaller. When it is highly miniaturized, the impedance Z will too high to obtain. In order to reach very small electrical length up to several degrees, the coupled line component was adopted. Since it is easy to get a highly impedance through choosing the even-mode impedance approximate to the odd- mode impedance. A diagonally shorted coupled lines and its equivalent circuit [21] are shown in Fig. 2.2.

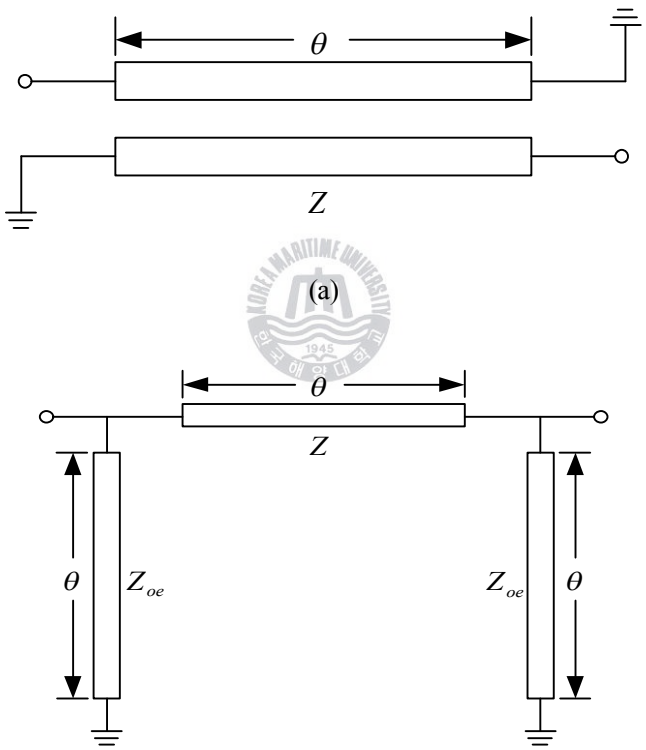

Fig. 2.2 Diagonally shorted coupled lines (a) and the equivalent circuit of the coupled lines (b).

The characteristic impedance of the diagonally shorted coupled lines can be represented by the even-mode and odd-mode characteristic impedance and thus is given by:

$$Z = \frac{2Z_{oe}Z_{oo}}{Z_{oe} - Z_{oo}} \tag{2.3}$$

Fig. 2.3 shows a shortened transmission line using Hirota's method with artificial resonance circuits. At the resonance frequency, the capacitance C_0 and the inductance L_0 cancel each other. So the equivalent circuit is the shortened quarter-wave transmission line using the Hirota's method as mentioned foregoing. At the resonance frequency, the following equation is satisfied:

$$\omega L_0 = \frac{1}{\omega C_0} \tag{2.4}$$

Compare the dotted box part in Fig. 2.3 and the equivalent circuit of the coupled lines in Fig. 2.2 (b). If the following equation is satisfied the dotted box part in Fig. 2.3 can be substitute by the equivalent circuit of the coupled lines. Then we get the substituted equivalent circuit as shown in Fig. 2.4.

$$\omega L_0 = Z_{oe} \tan\theta \tag{2.5}$$

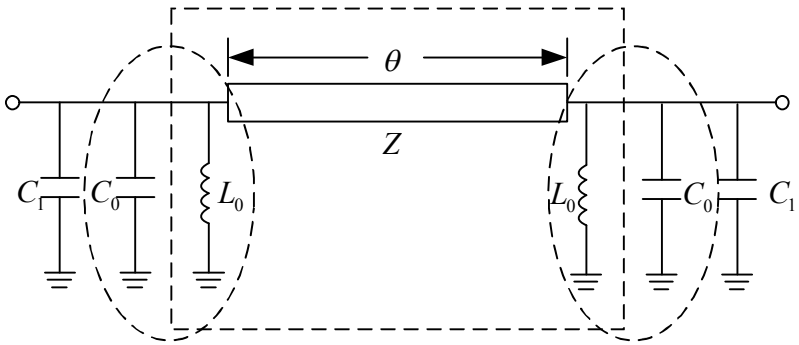

Fig. 2.3 A shortened transmission line with artificial resonance circuits.

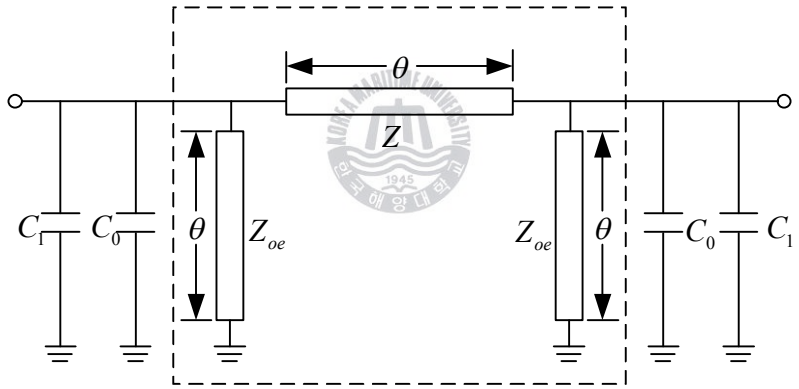

Fig. 2.4 The equivalent circuit substituted by the coupled lines' equivalent.

Finally, the two capacitors in each side of the Fig. 2.4 can combine mathematically, and the part in the dotted box is a diagonally shorted coupled line of Fig. 2.2 (a). The basic component of the filter can easily get. The structure of the diagonally miniaturized coupled lines with lumped capacitors appears as shown in Fig 2.5. And the relative equations

are as follows:

$$C = C_0 + C_1 \tag{2.6}$$

$$C_1 = \frac{\cos\theta}{\omega_0 Z_0} \tag{2.7}$$

$$C_0 = \frac{1}{\omega_0{}^2 L_0} = \frac{1}{\omega Z_{oe} \tan\theta} \tag{2.8}$$

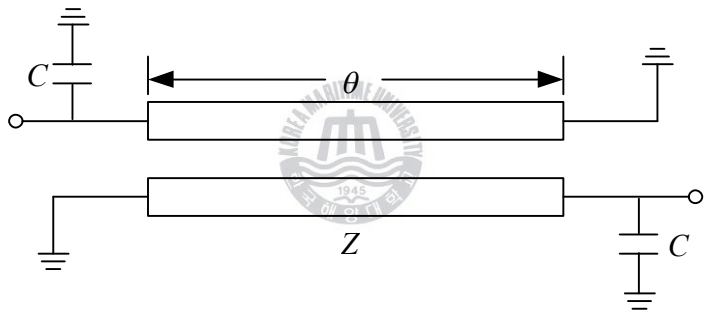

Fig. 2.5 The final equivalent circuit of the miniaturized quarter-wave transmission line.

This is the basic component of the proposed bandpass filter in this paper.

2.2 The one-stage filter

When design the filter, a capacitor was inserted between the input

and the output ports used to control the attenuation pole which located at the right of the center frequency. Since a mutual inductance appears due to the magnetic coupling between coupled lines, a series-parallel resonance composed of the center capacitor and the mutual inductor appears near the second harmonic frequency. But basically this attenuation pole can't be control without other components. A simple structure of the bandpass filter is shown in Fig. 2.6, in which the C_c is the inserted capacitor.

The capacitor C_c is used to control the attenuation pole which located at the right of the center frequency. The relation between the capacitance and the attenuation pole's location is researched using the HFSS software. The simulated result by HFSS software is plotted in Fig. 2.7. It shows that, the attenuation pole will move to the right as the capacitance increases. And the curve seems better. But if the capacitor is too large, in the higher frequency a peak will appear. So the capacitance has a limitation value. Using this capacitor, the curve shape can be optimized.

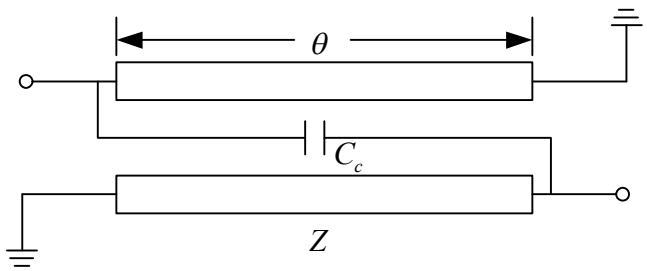

Fig. 2.6 The miniaturized coupled line bandpass filter with inserted capacitor between input and output ports.

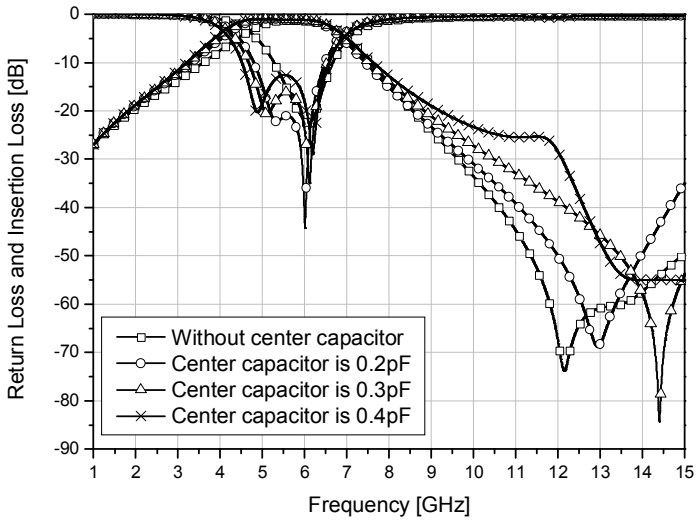

Fig. 2.7 The simulated results of the bandpass filter with different capacitance inserted to the input and output ports.

2.3 The quality factor enhancement method

The TSMC or MagnaChip CMOS procedure has 6 layers metal. Other types of CMOS procedure maybe has more or less metal layers. All of the metal layers can be used to make coupled lines to enhance the quality factor. In the next chapter, both the simulated and measured results will be plotted to show the different performances between the 6 layers coupled lines and single layer coupled line.

CHAPTER 3 The Simulation , fabrication and results analysis

In this chapter, the extraction procedure of quality factors from measurements of miniaturized coupled line bandpass filters will be described based on theoretical circuit analysis. And the Q factors of the designed filter will be compared with the filter which using a spiral inductor.

3.1 The quality factor extraction

The loss of the inductor is due to the series resistance. If we set the inductor is lossy and the capacitor is lossless. The equivalent circuit of the miniaturized transmission line in Fig 2.4 can be expressed as Fig. 3.1.

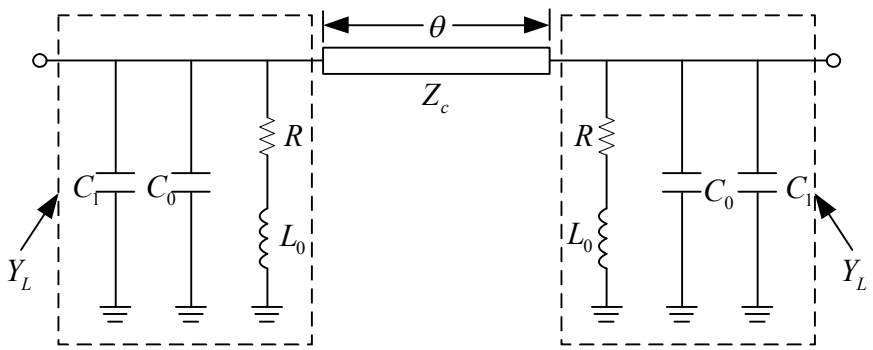

Fig. 3.1 The transmission line's equivalent circuit with lossy inductors.

The dotted box parts Y_L in both side of the equivalent circuit can be re-depicted in Fig. 3.2 by substituting the series resistance with shunt conductance.

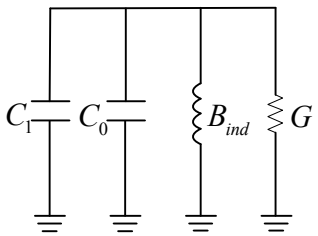

Fig. 3.2 The series resistance is substituted by the shunt conductance.

Where $$G = \frac{\alpha l}{Z_{oe} \sin^2 \beta l} \tag{3.1}$$

$$B_{ind} = Y_{oe} \cot \beta l \tag{3.2}$$

When resonance occurs, $B_{ind} = \omega_0 C_0$ is satisfied. And the capacitance C_0 cancelled with the inductance L_0 as known in Chapter 2. Then the total conductance of the equivalent circuit in Fig. 3.2 at resonance frequency is shown as:

$$Y_L = G + j\omega_0 C_1 \tag{3.3}$$

And then the form of the quality factor can be derived from (3.3) as follow:

$$Q = \frac{B_{ind}}{G} = \frac{Y_{oe}\cot\beta l}{\dfrac{\alpha l}{Z_{oe}\sin^2\beta l}} = \frac{1}{\alpha l}\frac{\cos\beta l}{\sin\beta l}\sin^2\beta l \approx \frac{\beta l}{\alpha l} = \frac{\beta}{\alpha} \tag{3.4}$$

The parameters α and β can be extracted from the measured parameters. From the Fig. 3.1, the entire *ABCD* matrix of the miniaturized quarter-wave transmission line is:

$$\begin{bmatrix} A & B \\ C & D \end{bmatrix}_T = \begin{bmatrix} 1 & 0 \\ Y_L & 1 \end{bmatrix} \begin{bmatrix} \cosh\gamma l & Z_C \sinh\gamma l \\ \dfrac{\sinh\gamma l}{Z_C} & \cosh\gamma l \end{bmatrix} \begin{bmatrix} 1 & 0 \\ Y_L & 1 \end{bmatrix} \tag{3.5}$$

Where $Y_L = j\omega C_1 + j\omega C_0 - j\dfrac{1}{\omega L_0} + G$

Regarding the short transmission line, the length is very small.

$\cosh\gamma l \approx 1, \sinh\gamma l = \gamma l = (\alpha + j\beta)l$ are satisfied. So we get:

$$\begin{bmatrix} \cosh\gamma l & Z_C \sinh\gamma l \\ \dfrac{\sinh\gamma l}{Z_C} & \cosh\gamma l \end{bmatrix} = \begin{bmatrix} 1 & Z_C(\alpha + j\beta)l \\ \dfrac{(\alpha + j\beta)l}{Z_C} & 1 \end{bmatrix} \tag{3.6}$$

$$\text{Put } Z_C(\alpha + j\beta)l = B_{TL} \tag{3.7}$$

$$\frac{(\alpha + j\beta)l}{Z_C} = C_{TL} \tag{3.8}$$

The entire *ABCD* matrix of the miniaturized quarter-wave transmission line is as follow:

$$\begin{bmatrix} A & B \\ C & D \end{bmatrix}_T = \begin{bmatrix} 1 & 0 \\ Y_L & 1 \end{bmatrix} \begin{bmatrix} 1 & B_{TL} \\ C_{TL} & 1 \end{bmatrix} \begin{bmatrix} 1 & 0 \\ Y_L & 1 \end{bmatrix}$$

$$= \begin{bmatrix} 1 + Y_L B_{TL} & B_{TL} \\ 2Y_L + C_{TL} + {Y_L}^2 B_{TL} & 1 + Y_L B_{TL} \end{bmatrix} \tag{3.9}$$

The *ABCD* matrix can know from the measured results. From (3.4) and (3.7), the Q factor can be calculated from the measured data. It is the ratio of the imaginary part and the real part of *B* parameter. Shown as follow:

$$Q = \frac{\beta}{\alpha} = \frac{Z_C \beta l}{Z_C \alpha l} = \frac{\mathrm{Im}(B_{TL})}{\mathrm{Re}(B_{TL})} = \frac{\mathrm{Im}(B_{measured})}{\mathrm{Re}(B_{measured})} \tag{3.10}$$

However, the measured *S21* of the fabricated BPF has an attenuation pole at high frequency [23], [24]. In practice, the Q-factor needs to be compensated for the attenuation generated from this magnetic inductor, as

seen in Fig. 3.3(a). The Q factor should be modified.

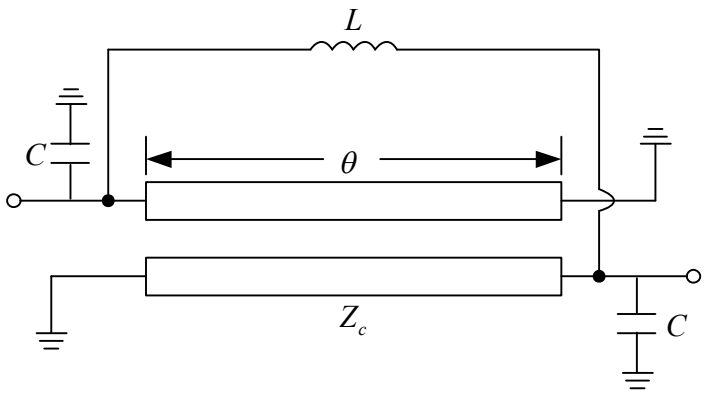

(a)

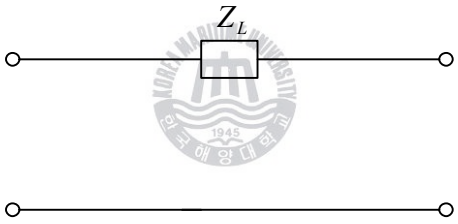

(b)

Fig. 3.3 (a) The equivalent circuit of the coupled line filter including the magnetic coupling inductor and (b) the equivalent circuit of the inductor.

The *ABCD* matrix of the inductor is:

$$\begin{bmatrix} A & B \\ C & D \end{bmatrix}_L = \begin{bmatrix} 1 & Z_L \\ 0 & 1 \end{bmatrix} = \begin{bmatrix} 1 & j\omega L \\ 0 & 1 \end{bmatrix} \tag{3.11}$$

And the *Y* parameter of the inductor can be calculated as:

$$[Y]_L = \begin{bmatrix} \frac{1}{Z_L} & -\frac{1}{Z_L} \\ -\frac{1}{Z_L} & \frac{1}{Z_L} \end{bmatrix} = \frac{1}{Z_L}\begin{bmatrix} 1 & -1 \\ -1 & 1 \end{bmatrix} \tag{3.12}$$

The *Y* parameter of the miniaturized coupled line can be calculated from (3.9).

$$[Y]_T = \begin{bmatrix} \frac{1+Y_L B_{TL}}{B_{TL}} & -\frac{1}{B_{TL}} \\ -\frac{1}{B_{TL}} & \frac{1+Y_L B_{TL}}{B_{TL}} \end{bmatrix} \tag{3.13}$$

So the total *Y* parameter of Fig. 3.3 (a) is as follow:

$$[Y'] = \begin{bmatrix} Y_{11}' & Y_{21}' \\ Y_{12}' & Y_{22}' \end{bmatrix} = [Y]_L + [Y]_T$$

$$= \begin{bmatrix} \frac{1}{Z_L} + \frac{1+Y_L B_{TL}}{B_{TL}} & -(\frac{1}{Z_L} + \frac{1}{B_{TL}}) \\ -(\frac{1}{Z_L} + \frac{1}{B_{TL}}) & \frac{1}{Z_L} + \frac{1+Y_L B_{TL}}{B_{TL}} \end{bmatrix} \tag{3.14}$$

And the total *ABCD* matrix can be expressed as:

$$\begin{bmatrix} A' & B' \\ C' & D' \end{bmatrix} = \begin{bmatrix} -\frac{Y_{22}'}{Y_{21}'} & -\frac{1}{Y_{21}'} \\ -\frac{|Y|}{Y_{21}'} & -\frac{Y_{22}'}{Y_{21}'} \end{bmatrix}$$

Since $B_{TL} = Z_C(\alpha + j\beta)l = Z_C\alpha l + jZ_C\beta l = \alpha' + j\beta'$

In this matrix

$$B' = -\frac{1}{Y_{21}'} = \frac{Z_L B_{TL}}{Z_L + B_{TL}} = \frac{X_L(-\beta' + j\alpha')}{\alpha' + j(X_L + \beta')}$$

$$= \frac{X_L\{\alpha' X_L + j[(\alpha')^2 + \beta'(X_L + \beta')]\}}{(\alpha')^2 + (X_L + \beta')^2}$$

Since $(\alpha')^2 = (Z_C\alpha l)^2 \approx 0$,

$$B' = \frac{X_L}{(X_L + \beta')^2}[\alpha' X_L + j\beta'(X_L + \beta')] = B_{measured} \quad (3.15)$$

where $B_{measured}$ is the *B* parameter of the measured *ABCD* matrix.

The ratio of the imaginary part and the real part of $B_{measured}$ parameter is:

$$\frac{\mathrm{Im}(B_{measured})}{\mathrm{Re}(B_{measured})} = \frac{\beta'(X_L + \beta')}{\alpha' X_L}$$

$$\text{So} \quad \frac{[\mathrm{Im}(B_{measured})]^2}{[\mathrm{Re}(B_{measured})]^2} = \frac{\beta'^2}{\alpha'} \times \frac{(X_L + \beta')^2}{\alpha' {X_L}^2} \tag{3.16}$$

From equation (3.15)

$$\frac{\beta'^2}{\alpha'} = \frac{\alpha' {X_L}^2}{(X_L + \beta')^2} \times \frac{[\mathrm{Im}(B_{measured})]^2}{[\mathrm{Re}(B_{measured})]^2} = \frac{[\mathrm{Im}(B_{measured})]^2}{\mathrm{Re}(B_{measured})} \tag{3.17}$$

$$\text{Where} \quad \beta' = Z_C \beta l = \frac{Z_0}{\sin\theta} \beta l \approx Z_0 \tag{3.18}$$

Since $r = \dfrac{(Z_0)^2}{50}$

Z_0 is derived from the measured data as follow:

$$Z_0 = \sqrt{50r} \tag{3.19}$$

where r is the input resistance at the center frequency which is a real number and can be known from the measured Smith Chart.

From the equations (3.17), (3.18) and (3.19) the modified Q factor is calculated as follow:

$$Q_{\mathrm{mod}} = \frac{\beta'}{\alpha'} = \frac{\beta'^2}{\alpha'} \times \frac{1}{\beta'} = \frac{1}{Z_0} \cdot \frac{[\mathrm{Im}(B_{measured})]^2}{\mathrm{Re}(B_{measured})} \qquad (3.20)$$

3.2 The experiment results of the Q factor

To examine the suitability of each equivalent circuit for the modeling of the measured results, the bandpass filters were fabricated with TSMC 0.18μm and MagnaChip 0.18μm process respectively. In order to compare the Q factors and to examine the Q enhance method, 1 layer and 6 layers circuit are fabricated with MagnaChip 0.18μm process. Fig. 3.4 shows the structures of miniaturized coupled coplanar bandpass filter, with 1 and 6 layers. For one layer circuit with the MagnaChip 0.18μm process, a coupled line of 7^o electrical length is used. The coupled line width is 20μm, the transmission line length is 570μm and the separation between the two coupled lines of 110μm is used to provide input/output impedance matching to the system impedance 50Ω. The six layer filter has a 20μm line width, 570μm line length, and 120μm coupled line separation.

These filters have been fabricated on a 10 Ω·cm bulk silicon substrate with aluminum metal layers. The total die area, including the ground plane surrounding the integrated BPF, is 700μm × 400μm. Coplanar coupled lines for the coupled line bandpass filter is used to avoid the coupling to other basic components in the transceiver system. Except for the input and output ports the ground plane is capsulated

around the filter. Photograph of the layout is shown in Fig. 3.5.

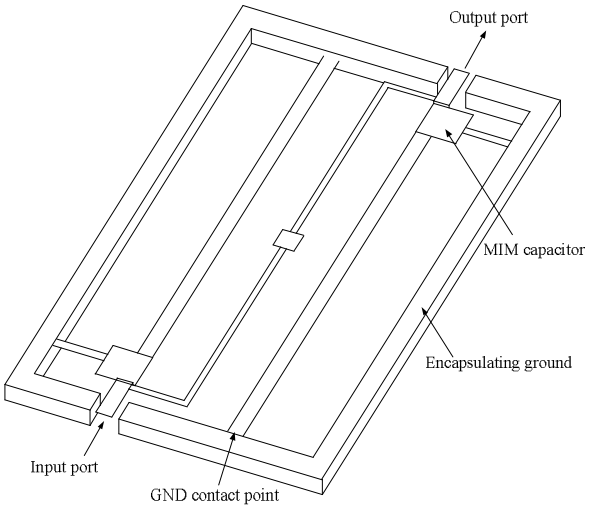

(a)

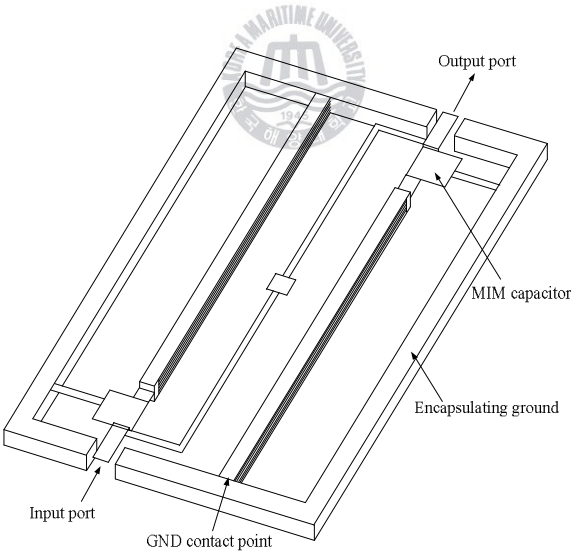

(b)

Fig. 3.4 (a) Miniaturized coupled line filter with 1 layer transmission line and (b) the filter with 6 layers transmission line.

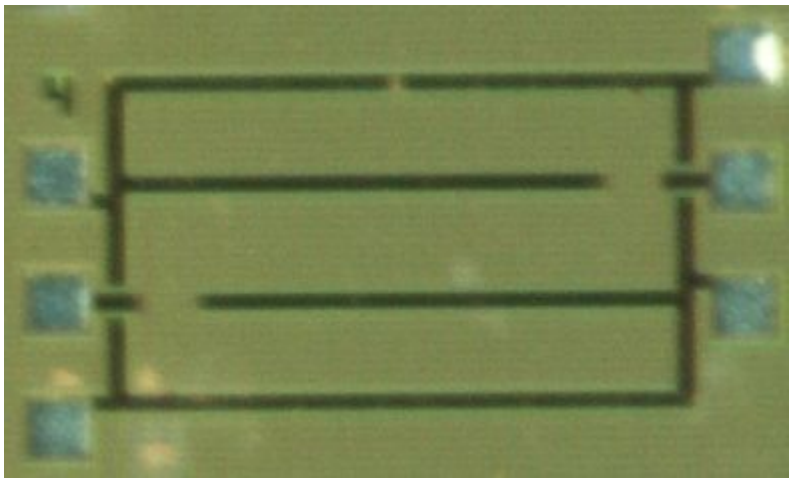

(a)

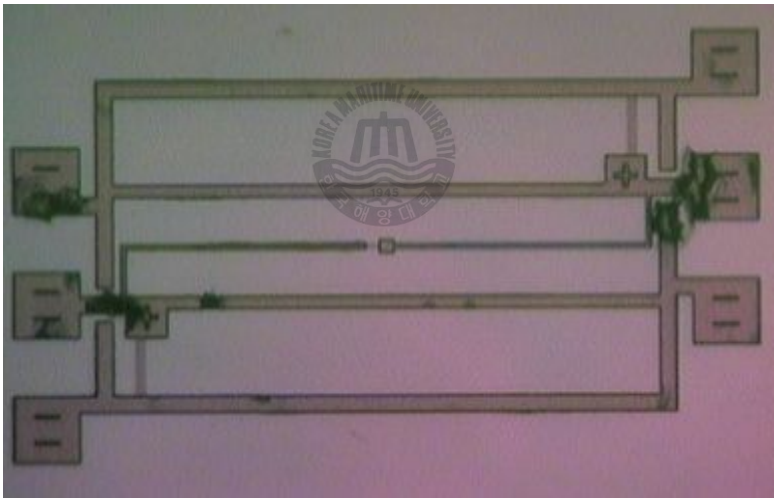

(b)

Fig. 3.5 (a) Photograph of the fabricated bandpass filter using MagnaChip 018 process and (b) the filter using the TSMC 018 process.

The measured *S11* and *S21* of the filter using MagnaChip 0.18μm process are plotted in one figure, as shown in Fig. 3.6. The insertion loss

of the 6 layer BPF at its resonant frequency of 4.8 GHz is -5.35 dB. This is an improvement of 1.9dB compared with the 1 layer BPF, which has an insertion loss of -7.27dB at resonance. Apparently, the BPF with 6 layers metal has advantage over the one with 1 layer.

The simulated and the measured results of the filter with 6 layers are plotted in one figure, as shown in Fig. 3.7, the simulated and the measured results are agree very well. The simulation is under the conditions, that the conductivity of the conductor is 0.1×10^7 S/m, because the conductivity goes smaller as the frequency goes higher, and the Si substrate conductivity is 10 Ohm·cm, that is in the most case.

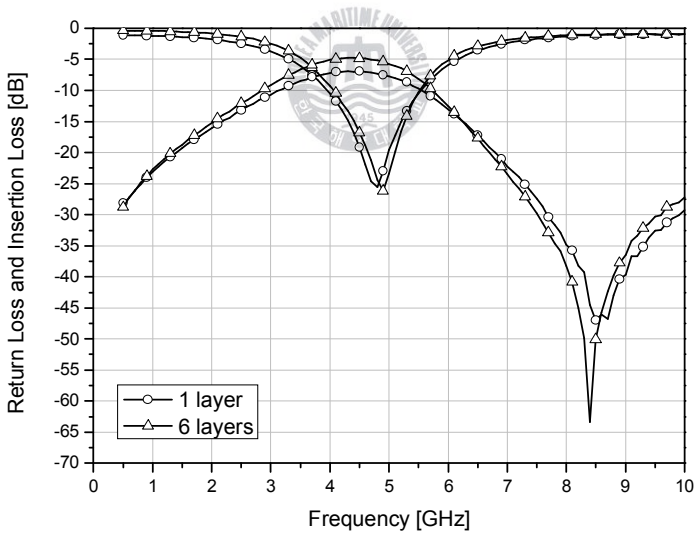

Fig. 3.6 The measured curves of the 1 layer and 6 layers bandpass filters.

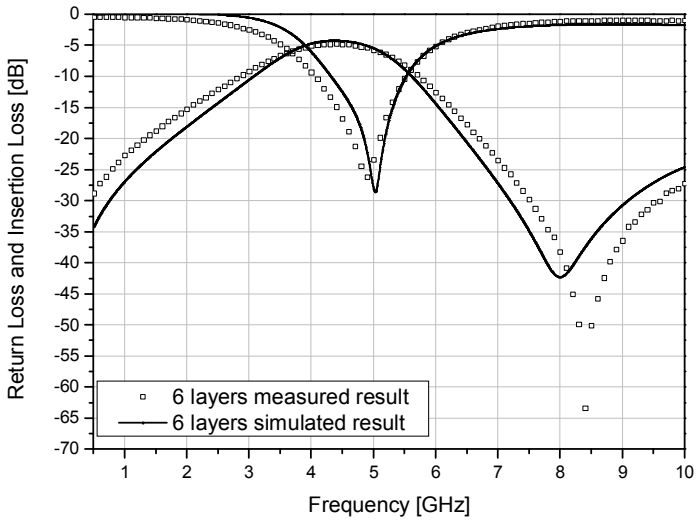

Fig. 3.7 The simulated and the measured results of the circuit with 6 layers coupled lines.

The attenuation constant is composed of the dielectric and conductive losses, as $\alpha = \alpha_c + \alpha_d$. Actually, the coupled coplanar transmission line is used in the CMOS process because grounding components does not require through-wafer via hole into the bottom ground beneath the substrate. The dielectric loss constant is described by [25]

$$\alpha_d = \frac{q\varepsilon_r \tan\delta}{\varepsilon_{eff}\lambda_g} \tag{3.21}$$

where ε_r is the relative dielectric constant of the substrate, ε_{eff} is the

relative effective dielectric constant of the guide, λ_g is the guide wavelength, and q is guide filling factor, expressed as $(\varepsilon_{eff}-1)/(\varepsilon_r-1)$. The conductive loss in the end-shorted stub with the characteristic impedance of Z_{oe} is given by [26],

$$\alpha_c = \frac{R_S\sqrt{\varepsilon_{eff}}}{K} \tag{3.22}$$

Where R_s is the surface resistivity of $\sqrt{\pi f \mu_0/\sigma}$ and K is a valuable involving the geometrical structure of coupled coplanar line. Notice that the substrate dielectric loss and conductive loss are both frequency dependent. But they operate in the different ways. The propagation constant β and substrate dielectric loss are simultaneously, inversely proportional to the frequency. In contrast, the conductive loss decreases proportionally with the square root of frequency as seen in (3.22). The simple quality factor in relation to the frequency is therefore shown by:

$$Q = \frac{k_1}{1(dielectric \cdot loss) + k_2/\sqrt{f}\,(conductor \cdot loss)} \tag{3.23}$$

Here, k_1 and k_2 are the relative constants and, specially, k_2 is a key factor that determines which of the dielectric of conductor loss is dominant. As an illustration of the frequency trend, Q-factor increase of CPW along with the frequency in the CMOS process was reported in [27]. It implied that the conductive loss in the CPW of the general CMOS process was still a relatively significant factor. It therefore gives the

intuitive insight that the thicker metal wires realized by connecting multiple metal layers in standard silicon technology can effectively improve the quality factor [28].

The ABCD matrix can be obtained from S-parameter measurements, from (3.10), the Q factor of 1 layer and 6 layers circuits are found to be 3.7 and 10.5 respectively. When the magnetic coupling inductor of Fig. 3.3 (a) is included in the calculations using equation (3.20), the Q factor of 1 layer circuit is found to be 4.5, and the Q factor of 6 layer circuit is found to be 11.4. These modified Q factors include the loss tangent of the dielectric of the shunt MIM capacitor in the resonator. Assuming the Q factor of the MIM capacitor to be 50 [29], the Q factors of the BPF on removal of this dielectric loss as found to be 4.9 and 14.8 for the 1 and 6 layer filters, respectively. Therefore, the effect of the multi-level implementation has been a Q factor improvement by a factor of around 3. Another BPF with 6 layers transmission line using TSMC 018 process was fabricated. And the Q factor is found to be 10.3 and the Q factor on removal of dielectric loss as found to be 12.

Many active bandpass filters employing spiral inductors have been developed but the performance are limited due to the low Q factors of the inductors. The performance of the fabricated filters are summarized in Tab. 1 and compared to other published RF active bandpass filters. As can be seen in Table 1, the Q factor of the distributed inductor in the bandpass filter with 6 layers is the highest yet reported when comparing with active BPFs using spiral inductors.

Table 1. Quality factor comparisons of BPFs implemented using the standard CMOS process.

Parameter	Unit	[30]	[31]	[32]	[33]	[34]	This work MagnaChip 1 layer	This work MagnaChip 6 layers	This work TSMC 6 layers
Technology	μm	CMOS 0.25	CMOS 0.18	CMOS 0.5	CMOS 0.8	CMOS 0.8	CMOS 0.18	CMOS 0.18	CMOS 0.18
Die area	mm^2	1.9	0.81	0.15	2.0	0.65	0.28	0.28	0.28
Filter order		6	4	4	4	2	4	4	4
3dB bandwidth	MHz	60	130	80	18	27.7	2500	2500	1500
Center frequency	MHz	2140	2030	1800	850	830	4800	4800	3850
Inductor Q		6	10*	2.7	3	3	4.9	14.8	12

*This is a simulation value and used a differential quality factor concept.

3.3 The stability of the center frequency

The equivalent circuit of the miniaturized coupled line as shown in Fig. 2.5 is shown in Fig. 3.8. The end-shorted shunt stub in Fig. 3.8 is a distributed inductor Z_{ind} for the shunt resonance circuit.

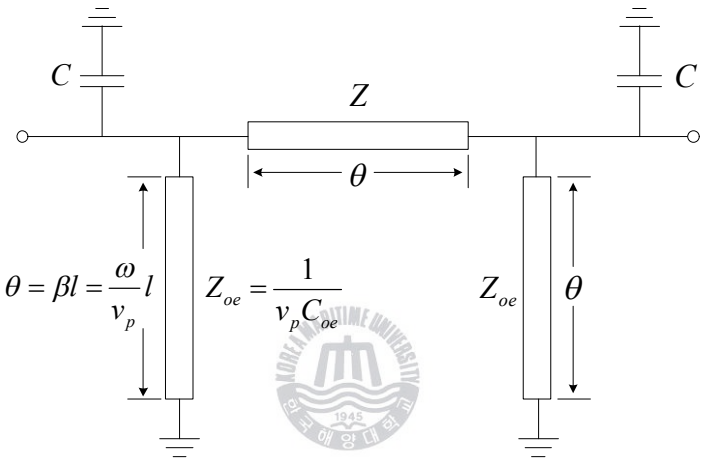

Fig. 3.8 A equivalent circuit of the miniaturized coupled line.

When the electrical length is very small, the distributed inductor is expressed by

$$Z_{ind} = jZ_{oe}\tan\theta = jZ_{oe}\theta = jZ_{oe}\frac{\omega l}{v_p} \tag{3.24}$$

The even mode impedance of a coupled coplanar waveguide is as follow [35],

$$Z_{oe} = \frac{60\pi}{\sqrt{\varepsilon_{eff}}} K' \tag{3.25}$$

where K' is a constant to be related to geometrical structure. In (3.24), v_p is expressed by

$$v_p = \frac{c}{\sqrt{\varepsilon_{eff}}} \tag{3.26}$$

In (3.24), the effective permittivity in the Z_{oe} and v_p are cancelled each other. The Z_{ind} is proven to be a constant regardless of the variations of the effective permittivity. Therefore, the dielectric materials' variation of oxide multi-layers in the fabrication procedure or effective dielectric change due to packaging do not make the center frequency of BPF swift at all.

In order to support the equation (3.24), the circuits with different substrates are simulated using HFSS. Fig. 3.9 shows the structure of the BPF. In the metal layers, the slot (the distance between the coupled lines) is 120μm and the gap (the distance from the coupled line to the ground) is 105μm. The width of the coupled line is 15μm. The HFSS simulation results of the BPF with different substrates are plotted in Fig. 3.10. Four kinds of substrates are used. The center frequency can easily be shown not to change when the relative dielectric constant under the silicon substrate shown in Fig. 3.9 changes. The results are agree well with the

phenomenon which expressed by the mentioned equations. The dielectric materials under the substrate and the circumstances of the integrated BPF, such as the package, hardly have an effect on the center frequency of highly miniaturized BPF.

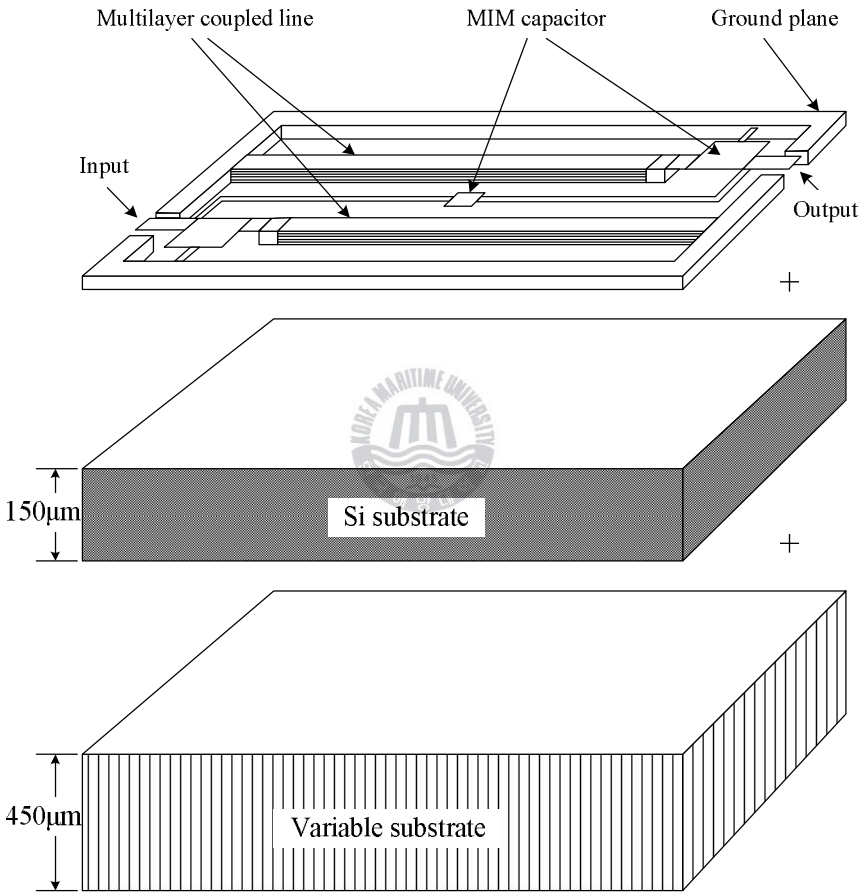

The "variable substrate" is with permittivity 41 material, permittivity 5.4 material, air or a thin metal ground respectively.

Fig. 3.9 The structure of the BPF with different substrates.

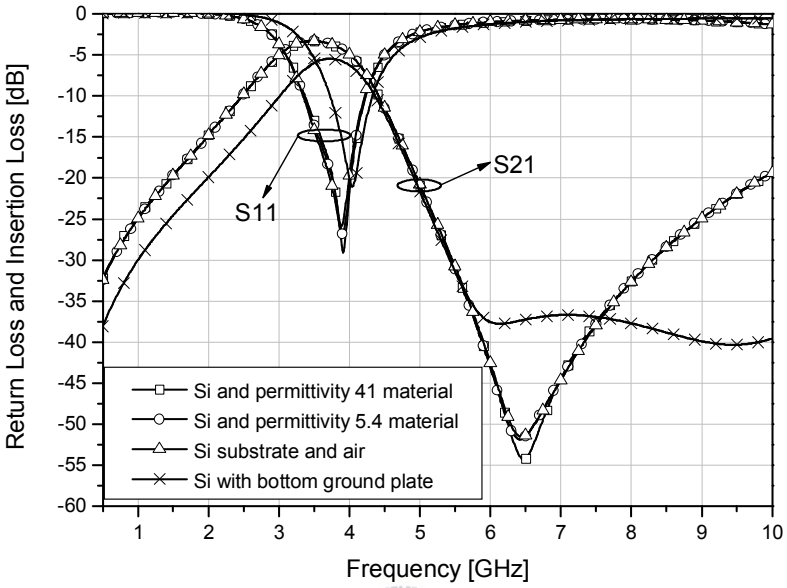

Fig. 3.10 The simulation results of the BPF with different substrate.

CHAPTER 4 Conclusion

A novel coupled lines bandpass filter are proposed in this paper. The proposed filter is based on the structure of capacitive loading of the parallel short-ended coupled-line, which is a relatively simple mean of reducing the coupled-line electrical length that usually plays a decisive role to the filter size. The proposed filter is a better way to solve the problem that the poor performance of on-chip active bandpass filters resulting from the low quality factor of monolithic spiral inductors. In addition, it was proven to have a relatively stable center frequency no matter how much the effective permittivity surrounding BPF changed. The dielectric materials' variation of oxide multi-layers in the fabrication procedure or effective dielectric change due to packaging do not make the center frequency of BPF swift at all. It demonstrated that the proposed BPF has a good feature which has a relatively stable center frequency for embedding into the transceiver chip. The methodology of quality factor extraction of distributed inductors from measurements of miniaturized, diagonally coupled line bandpass filters is presented.

The filters based on the TSMC CMOS and MagnaChip CMOS procedures were fabricated. Both single layer coupled line filter and 6 layers coupled lines filter are included. It is proved that the filter with 6 layers coupled lines has better performance than the one with only single layer coupled line. The insertion loss of the 6 layer BPF at its resonant frequency of 4.8 GHz is -5.35 dB. This is an improvement of 1.9dB

compared with the 1 layer BPF, which has an insertion loss of -7.27dB at resonance. The performance of the fabricated filters were compared with the other published RF active bandpass filters', the quality factor of 14.8 presented in this study is the highest published value for bandpass filter inductors implemented using the standard CMOS process. The quality factor of 14.8 achieved here is a good starting point and can be expected to further improve system noise figure, to the extent that it becomes comparable with that obtained when using off-chip filters. Following the trend within RFIC design to use copper conductors and to add further metal layers, this approach to on-chip BPF implementation is likely to become even more attractive and competitive in the future.

References

[1] S. J. Fiedziuszko, "Dual-mode dielectric resonator loaded cavity filters," *IEEE Trans., Microw. Theory Tech.*, vol. 82, no. 9, pp. 1311–1316, Sep. 1982.

[2] J. A. Curits and S. J. Fiedziuszko, "Miniature dual mode microstrip filters," *IEEE Trans., Microw. Theory Tech., Digest*, vol.2, pp. 443–446, Jul. 1991.

[3] C. Wang, K. A. Zaki, and A. E. Atia, "Dual-mode conductor-loaded cavity filters," *IEEE Trans., Microw. Theory Tech.*, vol. 45, no. 8, pp. 1240–1246, Aug. 1997.

[4] J. S. Hong and M. J. Lancaster, "Theory and experiment of novel microstrip slow-wave open-loop resonator filters," *IEEE Trans. Microw. Theory Tech.*, vol. 45, no. 12, pp. 2358–2365, Dec. 1997.

[5] J. S. Hong and M. J. Lancaster, "End-coupled microstrip slow-wave resonator filter," *Electronics Letters*, vol. 32, no. 16, pp. 1494-1496, 1 Aug. 1996.

[6] C. W. Tang, Y. C. Lin and C. Y. Chang, "Realization of transmission zeros in combline filters using an auxiliary inductively coupled ground plane," *IEEE Trans. Microwave Theory Tech.*, vol.51, no.10, pp.2112-2118, Oct,. 2003.

[7] A. Kundu and N. Mellen, "Miniaturized Multilayer Bandpass Filter with multiple Transmission Line Zeros", *IEEE MTT-S Int. Microwave Symp. Dig.*, pp. 760-763, June 2006.

[8] J. S. Hong and M. J. Lancaster, "Cross-coupled microstrip hairpin resonator filters," *IEEE Trans. Microw. Theory Tech.*, vol. 46, no. 1, pp. 118-122, Jan. 1998.

[9] J. T. Kuo and C. Y. Tsai, "Periodic stepped-impedance ring resonator (PSIRR) bandpass filter with a miniaturized area and desirable upper stopband characteristics" *IEEE Trans. Microw. Theory Tech.*, vol. 54, no. 3, pp. 1107-1112, Mar. 2006.

[10] J. T. Kuo and E. Shih, "Microstrip stepped impedance resonator bandpass filter with an extended optimal rejection bandwidth," *IEEE Trans. Microw. Theory Tech.*, vol. 51, no. 5, pp. 1554-1559, May. 2003.

[11] M. Makimoto and S. Yamashita, "Bandpass filters using parallel coupled strip-line stepped impedance resonators," *IEEE Trans. Microw. Theory Tech.*, vol. 28, no. 12, pp. 1413–1417, Dec. 1980.

[12] B. Dehlink, M. Engl, K. Aufinger, H. Knapp, "Integrated Bandpass Filter at 77GHz in SiGe Technology", *IEEE Microwave and Wireless Components Letters*, vol.17, pp346-348, May 2007.

[13] Y. Cao, R. A. Groves, X. Huang, N. D. Zamdmer, J. O. Plouchart, R. A. Wachnik, T. J. King, and C. Hu, "Frequency independent equivalent-circuit model for on-chip spiral inductors," *IEEE J. Solid-State Circuits*, vol. 38, no.3, pp. 419-426, Mar. 2003.

[14] J. N. Burghartz et al., "RF circuit design aspects of spiral inductors on silicon," *IEEE J. Solid-State Circuits*, vol. 33, pp. 2028-2034, Dec. 1998.

[15] C. P. Yue and S. S. Wong, "On-chip spiral inductors with patterned ground shields for Si-based RF ICs," *IEEE J. Solid-State Circuits*, vol. 33, No. 5, pp. 743-752, May 1998.

[16] A. Niknejad and R. Meyer, "Analysis, design, and optimization of spiral inductors and transformers for Si RF ICs," *IEEE J. Solid-State Circuits*, vol. 33, pp. 1470-1481, Oct. 1998.

[17] T. P. Wang and H. Wang, "High-Q Micromachined inductors for 10 to 30 GHz RFIC applications on low resistivity Si substrate", *Proc. of 36th European Microwave Conference*, pp. 56-59, 2006.

[18] X. He and W. B Kuhn, "A 2.5GHz low power, high dynamic range self tuned Q enhanced LC filter in SOI", *IEEE J. Solid-State Circuits*, vol. 40, No. 8, pp. 579-586, August 2005.

[19] S. B. Cohn, "Parallel-coupled transmission-line resonator filters," *IRE Trans.,* vol. MTT-6, no. 4, pp. 223-231, Apr. 1958.

[20] T. Hirota, A. Minakawa and M. Muraguchi, "Reduced-size branch-line and rat-race Hybrids for uniplanar MMIC's," *IEEE Trans. Microwave Theory Tech.*, vol. 38, no. 3, pp. 270-275, 1990.

[21] G. Matthaei, L. Young, E. M. T. Jones, *Microwave Filters, Impedance-Matching networks, and Coupling Structures*, Artech House, pp. 220.

[22] I. Kang, X. Wang, Y. Young, H. Zhang, "Theoretical analysis on attenuation of the 5GHz miniaturized GaAs MMIC bandpass filter", *Microwave Journal*, vol. 51. July, 2008.

[23] I. Kang, S. Shan, X. Wang, Y. Yun, J. Kim, C. Park, "A miniaturized GaAs MMIC filter for the 5GHz band", *Microwave Journal*, vol. 50, pp. 88-94, Nov. 2007.

[24] I. Kang, X. Wang, Y. Young, H. Zhang, "Theoretical analysis on attenuation of the 5GHz miniaturized GaAs MMIC bandpass filter", *Microwave Journal*, vol. 51. July, 2008.

[25] G. Chione, C. Naldi, and R. Zich, "Q-factor evaluation for coplanar resonators", *Alta Frequenza*, vol. 7, No.3, pp. 191-193, May. 1983.

[26] G. Chione and M.Goano, "A closed form CAD oriented model for the high frequency conductor attenuation of symmetrical coupled coplanar waveguides", *IEEE Microwave Theory and Technologies*, vol. 45, No.7, pp. 1065-1070, July. 1997.

[27] C. Doan, S. Emami, A. M. Niknejad, and R. W. Brodersen, "Design of CMOS for 60GHz application", *ISSCC Digest of Technical papers*, pp. 440-538, 2004.

[28] J. N. Burghartz, M. Soyuer, K. A. Jenkins, "Microwave inductors and capacitors in standard multilevel interconnect silicon technology", *IEEE Microwave Theory and Technologies*, vol. 44, No.1, pp. 100-104, Jan. 1996.

[29] J. N. Burghartz, M. Soyuer, K. A. Jenkins, "Microwave inductors and capacitors in standard multilevel interconnect silicon technology", *IEEE Microwave Theory and Technologies*, vol. 44, No 1, pp. 100-104, Jan. 1996.

[30] T. Soorapanth and S. S. Wong, "A 0dB IL ± 30MHz bandpass filter utilizing Q enhanced spiral inductors in standard CMOS", *IEEE J. Solid-State Circuits*, vol. 37, No. 5, pp. 579-586, May 2002.

[31] B. Georgescu, I. G. Finvers, and F. Ghannouchi, "2 GHz Q enhancement active filter with low passband distortion and high dynamic range", *IEEE J. Solid-State Circuits*, vol. 41, No. 9, pp. 2029-2039, Sept. 2006.

[32] A. N. Mohieldin, E. S. Sinencio, and J. S. Martinez, " A 2.7 V 1.8 GHz fourth order tunable LC bandpass filter based on emulation of magnetically coupled resonators", *IEEE J. Solid-State Circuits*, vol. 38, No. 7 pp. 1172-1181, July 2003.

[33] W. B. Kuhn, N. K. Yandura, and A. S. Wyszynski, "Q-enhanced LC bandpass filters for integrated wireless applications", *IEEE J. Solid-State Circuits*, vol. 46, No. 12 pp. 2572-2586, Dec. 1998.

[34] W. T. S Yan, R. K. C. Mak, and H.C. Luong, "2-V 0.8 μm CMOS monolithic RF filter for GSM receivers," *IEEE MTT Symp. Digest*, pp. 569-572, 1999.

[35] G. Ghione, M. Goano, "A closed-form CAD oriented model for the high frequency conductor attenuation of symmetrical coupled coplanar waveguides", *IEEE trans. Microwave theory and tech.*, vol. 45, NO. 7, July. 1997.

Acknowledgement

I would like to acknowledge many people who have helped me in both my study and daily life during the past two years. It is impossible for me to complete my study life without their supports and encouragements.

My greatest appreciation belongs to my advisor, Prof. In-Ho Kang. He is a creative and intelligent scholar. His strict research attitude and enthusiasm deeply impressed me. He taught me how to deal with problems, how to research new things. And I learned a lot from him in both science knowledge and working attitude which will influence my way to work and to study in the future. I feel very fortunate for his supervision and the words hardly express my gratitude to him. Without his help I couldn't complete my study in Korea.

I would also like to express my appreciation to the other professors of our department for their supports and guidance, who are Prof. Young Yun, Prof. Hyung-Rae Cho. Thanks for the supports and guidance on my paper and their help during the two past years.

I also want to thank the members of the other lab of our department because of the help on my study life. Specially, the heartfelt thanks are due to the past member of the RF Circuit & System Lab, Mr. Xu-Guang Wang, for lots of help and supports on the professional aspect.

Additionally, I want to thank all my friends in Korea Maritime University, for their unselfish help and emotional supports during the two years.

My special thanks belong to Prof. Ying-Ji Piao and Prof. Zong-Tao Chi at Qingdao University of China. Without their recommendation, it is impossible for me to get the opportunity to study in Korea.

Finally, my thanks would go to my beloved family for their continued love and strong supports throughout all these years. You are always the persons who believe in and encourage me in all my endeavors, which is a contributing factor to any success I may achieve. I feel great fortune to have you all accompany with me.